NANO LETTERS

pubs.acs.org/NanoLett

Molecular Origin of Fast Water Transport in Carbon Nanotube Membranes: Superlubricity versus Curvature Dependent Friction

Kerstin Falk,[†] Felix Sedlmeier,[‡] Laurent Joly,[†] Roland R. Netz,[‡] and Lydéric Bocquet*[,†]

[†]LPMCN, Université de Lyon, Université Lyon 1 and CNRS, UMR 5586; F-69622 Villeurbanne, France, and [‡]Physics Department, Technical University Munich, 85748 Garching, Germany

ABSTRACT In this paper, we study the interfacial friction of water at graphitic interfaces with various topologies, water between planar graphene sheets, inside and outside carbon nanotubes, with the goal to disentangle confinement and curvature effects on friction. We show that the friction coefficient exhibits a strong curvature dependence; while friction is independent of confinement for the graphene slab, it decreases with carbon nanotube radius for water inside, but increases for water outside. As a paradigm the friction coefficient is found to vanish below a threshold diameter for armchair nanotubes. Using a statistical description of the interfacial friction, we highlight here a structural origin of this curvature dependence, mainly associated with a curvature-induced incommensurability between the water and carbon structures. These results support the recent experiments reporting fast transport of water in nanometric carbon nanotube membranes.

KEYWORDS Carbon nanotubes, graphene, confined water, water transport, permeability, membranes, nanofluidics

Nanofluidics deals with the behavior of fluids in systems with nanometric sizes.[1,2] At such scales, fluid properties may be expected to strongly depart from what the frameworks of continuum approaches, for example, hydrodynamics, would predict, therefore allowing to bypass their limitations and open a broad range of novel perspectives. In this context, recent experimental works have put forward the potentially exceptional properties of carbon nanotube membranes in terms of water transport.[3−5] These membranes, made up of a macroscopic collection of hollow aligned carbon nanotubes (CNT) with diameters as small as 2 nm, were claimed to exhibit water flow up to 4 orders of magnitude faster than predicted by the hydrodynamic framework. This furthermore echoes the reported "soft dynamics" of water measured by neutron diffraction in single wall CNT with 1.4 nm diameter.[6] The reported fast water transport has raised great hopes to develop membranes with both high selectivity and high flux, reaching the efficiency of biological pores such as aquaporins,[7] with application for ultrafiltration or energy conversion.

However, up to now these results remain unexplained and their interpretation is controversial within state-of-the-art understanding.[8] Indeed, while low friction of water has been predicted and measured experimentally on hydrophobic surfaces,[2,9] the performance reached by the CNT membranes is orders of magnitude above the results measured up to now for "usual" (chemically modified) interfaces. This can be quantified in terms of the so-called slip length b measuring the liquid−solid friction; while b is on the order of tens of nanometers for water on hydrophobic surfaces,[2] the corresponding slip length for the CNT membranes would reach micrometers,[3] that is, far above usual expectations for slippage of water on hydrophobic surfaces. Furthermore, from the theoretical side, a number of works have specifically explored fluid flows in CNT using molecular dynamics simulations.[8,10−16] However numerical estimates of the slip lengths for water, extracted from velocity profiles, remain rather scattered and depend on the molecular model used for water so that no systematic conclusion or clear-cut interpretation could be drawn to explain the experimental results.[8] As an alternative explanation, one could also invoke the breakdown of continuum hydrodynamics at such scales as the origin of low friction, as is expected for single-file water transport in CNT.[12,16,17] However the experimental CNT membranes results in refs 3−5 were obtained for tubes with diameters above one nanometer in which deviations from bulk hydrodynamics are a priori expected to be minimal.[2,16] The physical mechanisms at the origin of the reported fast flows thus remain fully open within the state-of-the-art, leaving uncertain the potential applications at stake.

Our aim in this work is therefore to assess on theoretical grounds the unique properties of CNT membranes for water transport, to validate or refute the previously reported experimental results, and to give a general framework for the specific water transport in CNTs. To this end, we carried out a systematic exploration of the liquid/solid friction of water on planar graphitic surfaces as well as inside and outside single carbon nanotubes, using both molecular dynamics simulations and theoretical analysis. Altogether,

* To whom correspondence should be addressed. E-mail: lyderic.bocquet@univ-lyon1.fr.

Received for review: 06/15/2010
Published on Web: 09/16/2010

DOI: 10.1021/nl1021046 | *Nano Lett.* **2010,** *10,* 4067–4073

our results do indeed confirm that CNTs act as fast water transporters, pointing to an unforeseen mechanism at the origin of the ultralow water−carbon friction. Several key results emerge from our study: (i) we report a strong curvature dependence of the water−graphite friction, decreasing for water inside CNT, increasing for water outside, while independent of confinement for water in a planar graphene slab; (ii) this leads as a paradigm to superlubricity of water below a threshold diameter, characterized by a vanishing friction coefficient, that is, unmeasurable friction; (iii) the main physical mechanism at the origin of this phenomenon is a curvature-induced incommensurability of the water structure with respect to the carbon matrix; (iv) the predicted flow enhancement is on the order 10^3-10^4 for CNTs with diameters in the range of 1−2 nm and $\sim 10^1$ for diameters of order 50 nm, both in agreement with the experimental results by (respectively) Holt et al.[4] and Whitby et al.[5] under similar conditions. A dependence of the slip length on CNT radius was first reported numerically by Thomas and McGaughey[8] for water inside a tube; while our results confirm this tendency, our exhaustive analysis of water friction provides a thorough microscopic understanding, pointing to a specific curvature-induced friction weakening, independent of the specific water molecular model. Altogether, our results constitute a "proof-of-principle" for the outstanding performance of carbon nanotube membranes.

MD Simulations of Water−Carbon Friction. The friction of liquids on solid surfaces is usually discussed in terms of the partial slip hydrodynamic boundary condition that relates the fluid velocity v_{slip} at the solid surface to its gradient $\partial_n v$ in the direction normal to it as $b\partial_n v = v_{slip}$, where b is the slip length.[9] While various numerical studies have quantified slippage of water in CNTs by measuring directly the velocity profiles at the surface, this approach becomes inefficient when b is substantially larger than the confinement. Indeed the velocity profile tends to a plug, leading to large uncertainties in the values of the slip length. In this work, we have thus taken a different approach and focused on the liquid/solid friction coefficient of water at graphitic surfaces.

Indeed, the partial slip boundary condition stems physically from the identification of the "bulk" viscous stress $\sigma_f = \eta\partial_n v$ (η the shear viscosity) with a surface fluid−solid friction force, $F/\mathcal{A} = -\lambda v_{slip} = -\sigma_f$, with λ the fluid/solid friction coefficient and $\mathcal{A}$ the contact area. The slip length is accordingly deduced from the liquid/solid friction coefficient λ by the relation $b = \eta/\lambda$. The friction coefficient is the physically relevant property characterizing the interfacial dynamics, a large slip length being associated with a low friction. As any dissipation coefficient, the friction coefficient can be expressed via linear response theory in terms of a Green−Kubo (GK) relationship, relating λ to a correlation function of a fluctuating microscopic variable at equilibrium[9]

$$\lambda = \frac{1}{\mathcal{A}\, k_B T}\int_0^\infty \mathrm{d}t \langle F(t)F(0)\rangle_{equ} \qquad (1)$$

where $F(t)$ is the total tangential force acting along the axial direction on the surface with area $\mathcal{A}$ and the average runs over equilibrium configurations.

In this study, we have therefore performed both equilibrium and nonequilibrium molecular dynamics simulations of water in graphitic channels. Two independent approaches were followed to extract the friction coefficient λ: (i) from pressure driven flows, as the ratio between the friction force of water at the surface and the slip velocity, $\lambda = -F/\mathcal{A}v_{slip}$; and (ii) in equilibrium (flow-free) situations with λ being calculated from the GK relationship in eq 1.

To get insight into the physical mechanisms at play, we have explored various geometries and topologies, as sketched in Figure 1. We have simulated water flowing inside and outside single-walled CNT (along the tube axis) with diameter ranging from 20.4 down to 0.68 nm, Figure 1a−c. CNT with both armchair and zigzag chiralities were considered. To disentangle the roles of confinement and topology, we have also considered a slab geometry with water confined between two parallel graphene sheets with width varying between 6.11 and 0.68 nm. Following Hummer et al.,[12] we used the AMBER96 force field[18] with TIP3P water and water−carbon interactions modeled by a Lennard-Jones potential between oxygen and carbon with parameters $\varepsilon_{OC} = 0.114$ kcal/mol and $\sigma_{OC} = 3.28$ Å. To assess the generality and robustness of the results, we have furthermore conducted several simulations using the SPC/E model of water, with a Lennard-Jones interaction between oxygen and carbon atoms,[19] fitted to reproduce the experimental wetting properties of water on graphite. The contact angle of water on a planar graphene layer for these two models, which we measured independently, are $\theta = 57°$ for TIP3P and $\theta = 95°$ for SPC/E. While graphitic planar surfaces are supposedly hydrophobic (the contact angle of water on HOPG is typically around 86°), experiments show that water intrudes the CNTs down to the smallest diameters.[4,6]

In the following text, we will mainly discuss the results for the TIP3P water model, while the SPC/E results are reported in Supporting Information. Most of the simulations were carried out with the LAMMPS molecular dynamics package,[20] but we also used GROMACS[21] as a comparison. Long range Coulombic forces were computed using the PPPM method; a time step of 2 fs was used and typically, simulations of a few nanoseconds were performed.

To ensure equal lateral pressure for all tube sizes, the CNT with water inside were initially connected to two reservoirs at both ends, whose pressure was set to 1 atm with a piston. The reservoirs were then removed, and periodic boundary conditions were imposed along the tube axis. For computational efficiency, we used a different procedure with the graphene slabs; one of the graphene sheets was first used as a piston to

DOI: 10.1021/nl1021046 | Nano Lett. 2010, 10, 4067--4073

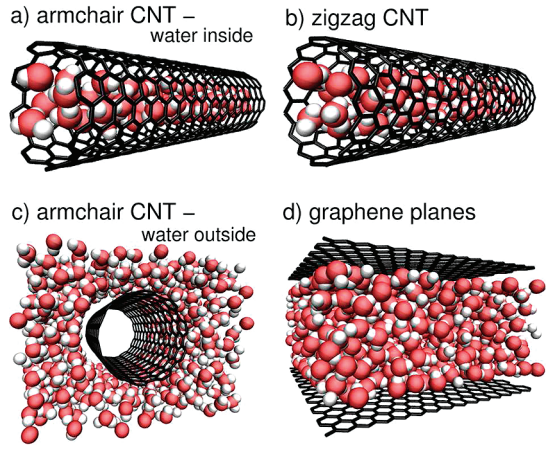

FIGURE 1. Systems considered in this study. Flow of water inside armchair (a) and zigzag (b) CNT, outside armchair CNT (c), and between graphene sheets (d).

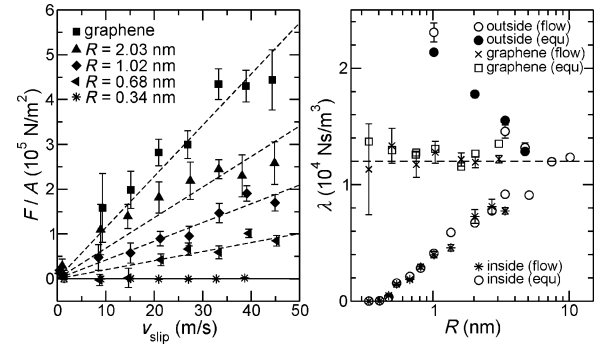

FIGURE 2. (a) Friction force of water versus slip velocity at the carbon nanotube surface for various confinements inside the CNT. The top result is for the graphene slab (with wall-to-wall distance $h = 3.23$ nm). (b) Evolution of the friction coefficient λ with the confinement R, for water inside/outside CNT (with a diameter $d = 2R$) and between graphene sheets (at a distance $H = 2R$). Flow measurements: graphene ($\times$); armchair CNT, inside (*) and outside (○). Equilibrium measurements: graphene (□); armchair CNT, inside (○) and outside (●). Otherwise indicated, uncertainties are on the order of symbol size.

impose the required pressure, and then fixed at its average equilibrium position for flow measurements. Water molecules were kept at a constant temperature of 300 K using a Nosé–Hoover thermostat, applied only to the degrees of freedom perpendicular to the flow with a damping time of 200 fs. The positions of the carbon atoms were fixed.[28]

In the nonequilibrium simulations, Poiseuille flows were driven by applying a constant acceleration $a_0 \sim 10^{-4}$nm/ps^2 to all O and H atoms (corresponding to a pressure gradient $\sim 10^{14}$ Pa/m, a driving force similar or lower than in previous works[8,15]). Because of the very large slippage at the surfaces, velocity profiles are flat (pluglike) over the channels' width. The slip velocity v_{slip} is defined as the fluid velocity within the first water layer close to the surface. But due to the flat velocity profiles, the slip velocity can be identified in most cases with the average fluid velocity. In parallel, one measures the friction force F acting on the carbon structure and due to the water molecules. During a simulation, both the friction force F and slip velocity v_{slip} increase over very long time scales (approximately nanoseconds), to finally reach a stationary state. However, as a consequence of the low liquid/solid friction, this relaxation time is much larger than the momentum diffusion transfer time scale associated with the building up of the flow profile, and one may consider this relaxation as a quasi-stationary state. We thus take benefit of this time-scale separation by measuring the force–velocity relationship in a single simulation within such a quasi-stationary regime. Statistical uncertainties were estimated by repeating this procedure for ~20 different initial configurations. In Figure 2a, we show the result of this procedure, leading to a linear relationship between the friction force and the slip velocity. Nonlinear deviations are observed for v_{slip} above ~50 m/s.

The friction coefficient was also determined using eq 1 in equilibrium simulations. The value of λ is obtained from the plateau of the integrated force autocorrelation function, occurring typically in the range $t \in$ [1 ps;10 ps]. A well-documented difficulty of such equilibrium estimates of GK relationships is associated with the finite size of the simulated system, which leads after a very long time-scale to a vanishing of the friction coefficient due to an inversion of infinite time and thermodynamic limit.[22,23] However this decay of the time integral occurs on very long time scales (here, typically nanoseconds) and a plateau value can be defined over intermediate times in the picosecond range (see Supporting Information), thereby avoiding this spurious long time effect. In the following, we take this plateau value as the equilibrium value for the friction coefficient. We checked that both equilibrium and nonequilibrium estimates of λ do match, see Figure 2b.

A few further remarks can be made. First, in the case of graphene sheets, friction is measured to be independent of the orientation. Finally, results for λ were found to be qualitatively and semiquantitatively similar for the two considered models of water, TIP3P and SPC/E, with a qualitatively similar dependence on curvature (see Supporting Information). This demonstrates the robustness of the reported effect.

Curvature Dependent Friction Coefficient. In Figure 2b, we gather the results for the friction coefficient in the different geometries considered, as a function of the confinement R (nanotube radius or half width for the graphene slab). The first key result highlighted by this plot is that the friction coefficient λ is strongly dependent on the curvature of the graphitic surface: it decays with CNT radius for positive curvature (water inside nanotubes), but increases for negative curvature (water outside nanotubes). In contrast the friction coefficient for the graphene slab (with zero curvature) does not depend on the confinement, confirming that the curvature is the relevant parameter controlling friction. A second key conclusion is that the friction coefficient vanishes within numerical uncertainty below a threshold

DOI: 10.1021/nl1021046 | Nano Lett. 2010, 10, 4067–4073

radius ($R_c \approx 0.4$ nm), leading to a "superlubric" behavior of water. Another remarkable feature to be noted from Figure 2 is that the friction coefficient deviates significantly from its low confinement, flat surface, value ($R \rightarrow \infty$) already for CNT's diameters below ~10 nm. The occurrence of an effect at such "large" confinements (with respect to water structure) is quite puzzling.

To give orders of magnitude, these results may be also discussed in terms of corresponding slip lengths. Using the bulk value for the viscosity of water,[29] one gets a slip length $b \approx 80$ nm for water on graphene surfaces for both TIP3P and SPC/E models. But in CNTs with a diameter of 1 nm, the MD results in Figure 2 lead to $b \approx 500$ nm, close to the result by Holt et al. in the same conditions.[4] For a diameter of 7 nm, we find a slip length $b \approx 120$ nm, substantially smaller than the experimental result of Majumder et al.,[3] and our numerical findings compare more favorably with Holt et al.'s experimental results. Note that these values are much larger than the ones measured for water on diamondlike surfaces.[24] This is due to the smooth nature of the graphene surface. As a further remark, we note that while these values of b for both TIP3P and SPC/E models differ quantitatively from those by Thomas and McGaughey using a different model (TIP5P for water together with the parameters of Werder et al. for oxygen−carbon interaction),[8] reporting $b \approx 30$ nm for planar graphene slabs, a qualitatively similar behavior of b with CNT radius is reported for water inside CNT.

These results provide a strong support for the reported experimental behavior. But such huge values of slip length on molecular surface cannot be accounted for under the usual interpretations of nanometric slippage based on hydrophobic effects.[9,24]

Toward a Microscopic Understanding of the Curvature Effect. To understand the origin of the observed very strong curvature dependence of the friction coefficient, we have explored a number of possible factors that could affect friction. We have in particular considered the effects on the water-CNT friction of wetting, pressure, water structure, and interfacial depletion of water at the CNT surface, which are usually known to affect slippage on hydrophobic surfaces.[24] However, our simulations showed that presently, none of these factors are responsible for the measured effect.

To be more specific, we showed (see Supporting Information) that

(i) Results were qualitatively and semiquantitatively equivalent for the two water models considered, that is, TIP3P and SPC/E, while exhibiting quite different contact angles on graphene ($\theta = 57°$ and $\theta = 95°$, respectively);

(ii) The friction coefficient on the graphene surface was found to be independent of pressure in the interval [−1000; +500] atm. We checked independently that the difference between normal and tangential pressure at curved water/CNT interfaces ranges in a similar interval of [−1000;0] atm.

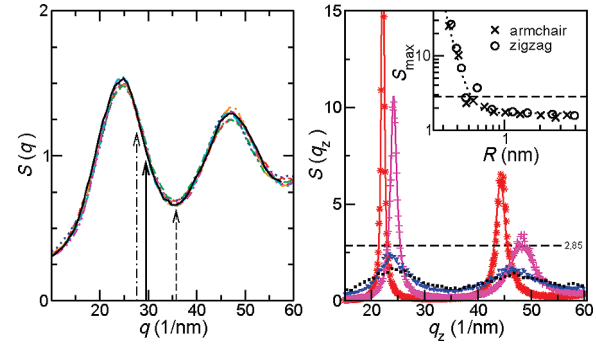

FIGURE 3. (a) Structure factors $S(q)$ of water in the first layer close to the carbon surface, for the slab geometry and six armchair CNTs with radii in the range 0.81−3.39 nm. Results for the various CNT radii are found to superimpose. The arrows indicate the range of variation for the curvature dependent wave-vector $|\tilde{q}_{\pm}|$ characterizing the carbon−water energy landscape (see text): solid arrow, planar surface ($R \rightarrow \infty$); dashed arrow, water inside a CNT with radius 0.8 nm; dashed-dot arrow, water outside a CNT with radius 0.8 nm. (b) Structure factor of water with wave vector q_z along the CNT length, for graphene (black) and within the smallest CNTs (blue, $R = 0.475$ nm; magenta, $R = 0.407$ nm; red, $R = 0.339$ nm). The lines correspond to a simplified 1D analytical model of the water structure (see Supporting Information for details). Inset: Maximum value of the structure factor, measured at its first peak. The horizontal line with $S_{max} = 2.85$ defines the onset of water crystallization.

(iii) The density profile of water in the first layer at contact with the graphitic surface (within approximately one oxygen diameter close to the surface; see Supporting Information) barely varies when the curvature is changed. This can be quantified by a depletion length[24] measuring the excess density at the interface; the latter is found to vary between 0.17 and 0.18 nm for CNT radii in the range [1 nm;5 nm], thus showing no correlation with friction in this radii range.

(iv) The structure of water is not affected by confinement for CNT radii above 0.8 nm. This is demonstrated in Figure 3a where the structure factor of oxygen atoms in the first water layer close to the surface is shown for various CNTs' radii. Again, the water structure is not found to correlate with the friction factor decrease, the latter being already significant for large tubes. We furthermore checked that in this weak confinement regime the structure factor remains isotropic.

Only in the smallest tubes with $R < 0.5$ nm is the water structure influenced by the confinement, as exhibited in Figure 3b. For these smallest tubes, water displays a single-file structure, in agreement with previous studies.[12,16,17] The change in structure can be quantified by the maximum value of the structure factor, S_{max}. As shown in Figure 3b, this value remains constant down to the smallest tubes and starts to increase only for $R < 0.5$ nm. Water crystallization, probed here by a Hansen−Verlet criterion $S_{max} > 2.85$,[25] is found only for the smallest CNT with single file water.

This suggests the existence of two regimes for water in CNT: a weak and a strong confinement regime, the transition occurring for CNT radius $R \approx 0.5$ nm, which is in agreement with the results of ref 16. The vanishing of the friction

DOI: 10.1021/nl1021046 | Nano Lett. 2010, 10, 4067–4073

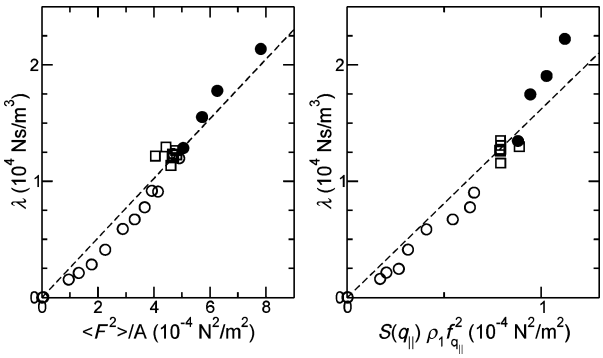

FIGURE 4. (a) Functional dependence of the friction coefficient λ versus the static rms force $\langle F^2 \rangle$. This plot gathers results for all confinements and geometries: ○, water inside CNT; ●, water outside CNT; □, water inside a planar graphene slab. (b) Functional dependence of the friction coefficient λ on the structural parameter characterizing the water structure at the graphitic interface (see text for definitions). Dashed lines are guides to the eye.

coefficient occurs in the strong confinement regime (radii below 0.5 nm), where a strong structuration of water builds up inside the tube, see Figure 3b, together with an important smoothing of the water−carbon energy landscape, as we demonstrate below in Figure 5. However, the fact that friction strongly decreases already in the weak confinement regime is fully unexpected.

Microscopic Description of Friction. To get further insight, one may consider the GK expression for the friction coefficient in eq 1. This expression may be first rewritten formally as $\lambda = 1/(\mathcal{A} k_B T) \langle F^2 \rangle \times \tau_F$, defining the decorrelation time τ_F characterizing the decay of the force−force autocorrelation function, $\tau_F = \int_0^\infty dt \langle F(t)F(0) \rangle / \langle F^2 \rangle$. Interestingly this time depends only very weakly on the CNT curvature in the weak confinement regime (Supporting Information). It is typically on the order of 100 fs (see Supporting Information, Figure 5a,b). In contrast, the variation of the friction coefficient λ on CNT curvature is found to directly correlate with the static rms force $\langle F^2 \rangle$, as shown in Figure 4a, both for water inside ("positive" curvature) and outside ("negative" curvature) the tubes. This points to a static origin of the curvature effect and discards a dynamic origin even though, as pointed out above, the structure of water is not affected by confinement in this regime.

rms Force for Water at a Flat Graphene Surface. An analytical estimate of the rms force $\langle F^2 \rangle$ can be obtained for weak confinements. Let us first consider the corrugated energy landscape felt by one water molecule on a (flat) graphene layer. Expanding in Fourier space, this may be written $\mathcal{V}(\mathbf{x}_{||}, r_\perp) = \mathcal{V}_0(r_\perp) + \mathcal{V}_1(r_\perp)(\cos(\mathbf{q}_- \cdot \mathbf{x}_{||}) + \cos(\mathbf{q}_+ \cdot \mathbf{x}_{||})) + \ldots$, where $\mathbf{x}_{||}$ and $r_\perp$ are the coordinates parallel and perpendicular to the graphene surface. For the hexagonal structure, the $\mathbf{q}_\pm$ vectors, along the graphene plane, are $\mathbf{q}_\pm = q_0(1/\sqrt{3}; \pm 1)$ with $q_0 = 2\pi/\ell_0$ and ℓ_0 the distance between hexagon centers ($q_0 \simeq 25.5$ nm^{-1}); see Supporting Information. Following ref 26, one may rewrite the total (fluctuating) force in a direction z parallel to the graphene layer as $F(t) = \int d^3\mathbf{r} f_z(\mathbf{x}_{||}, r_\perp) \hat{\rho}(\mathbf{x}_{||}, r_\perp)$, where $\hat{\rho}(\mathbf{x}_{||}, r_\perp)$ is the density operator and $f_z = -\nabla_z V$ is the force density along z. The main contribution to the force comes from the first water layer at the interface and after some straightforward calculations, one may obtain the total rms force as

$$\langle F^2 \rangle / \mathcal{A} = \frac{1}{2} \rho_1 f_{q_{||}}^2 (S(q_+) + S(q_-)) \qquad (2)$$

with $f_{q_{||}} = q_0 \mathcal{V}_1(r_0)$ (r_0 is the position of the first peak of the water profile), and ρ_1 is the surface density of water molecules in the first layer; $S(q_\pm)$ is the structure factor of water in the first layer [$S(q) = \langle \hat{\rho}_q \hat{\rho}_{-q} \rangle_{1\text{st layer}}$ where $\hat{\rho}_q$ is computed only in the first layer[26]] along the wave-vectors $q_\pm$ with $|q_\pm| \simeq 29.5$ nm^{-1}; see Figure 3.

rms Force for Water at a Curved Graphitic Surface. Now, coming back to the problem of water−CNT interface, we can map the curved geometry to the above planar situation by unrolling the first layer of water close the CNT onto a planar graphene plane. Note that this procedure is of course valid only in the weak confinement regime where a first layer can be defined (typically for $R > 0.6$ nm). In practice, this is conveniently done by using cylindrical coordinates of the water molecules in the first layer and of the CNT carbon atoms; it amounts to replacing in the above Fourier expansion of the force the $\mathbf{q}_\pm \cdot \mathbf{x}_{||}$ terms by their angular equivalent in cylindrical coordinates $q_\phi \cdot \phi + q_0 \cdot z$, with $q_\phi = \pm q_0 \times R/\sqrt{3}$ as the angular reciprocal wave vector of the curved CNT (R the CNT radius). Now, in the equivalent unrolled structure, the coordinate x of water molecules in the first layer relate to ϕ according to $x = r_0 \cdot \phi$ (with r_0 the radial position of the first water layer). One then deduces the energy landscape for water at the curved interface with the lateral modulation which is now given by $\tilde{\mathbf{q}}_\pm \cdot \mathbf{x}_{||}$ with $\tilde{\mathbf{q}}_\pm$ a curvature dependent wave-vector defined as $\tilde{\mathbf{q}}_\pm = q_0\{R/r_0 \times 1/\sqrt{3}; \pm 1\}$.

Finally, following the same approach as above, this leads to an equivalent rms force as in eq 2, but with both $S(q)$ and $f_{q_{||}}$ terms calculated at the curvature dependent wave-vector $\tilde{\mathbf{q}}_\pm$. Note that in curved CNT, the position of the first water peak is typically $r_0 \simeq R \pm \sigma_{OC}$ ($\pm$ for water outside/inside CNT). A key remark is that, while the structure factor of water remains merely unchanged in weak-confinement (see Figure 3a), it is computed at an R dependent wave-vector, $\tilde{\mathbf{q}}_\pm$, leading *in fine* to large variations of the friction coefficient versus R. In Figure 3a, the arrows indicate the range of variation of the $\tilde{q}_{||}$ wave vector for water inside and outside the CNTs.

Curvature Effects on the Friction Coefficient. Altogether the above description predicts a friction coefficient taking the form

DOI: 10.1021/nl1021046 | *Nano Lett.* **2010,** *10,* 4067–4073

$$\lambda \approx \frac{\tau_F}{k_B T} \times \rho_1 \tilde{f}^2_{q_{||}} S(\tilde{q}_{||}) \qquad (3)$$

with $S(\tilde{q}_{||}) = S(\tilde{q}_+) = S(\tilde{q}_-)$ the water structure factor, computed at a wave vector $\tilde{\mathbf{q}}_\pm = q_0\{R/r_0 \times 1/\sqrt{3}; \pm 1\}$, $r_0 \simeq R \pm \sigma_{OC}$ ($\pm$ for water outside and inside, respectively), and τ_F merely independent of R.

To assess this picture, we have checked this relationship by computing each term of the right hand side of eq 3. The water structure factor is measured in simulations (Figure 3); $\tilde{f}_{q_{||}}$ is calculated from the direct estimate of the force density acting on a single water molecule inside or outside a CNT with given radius R, at the position of the first water layer r_0; finally, ρ_1 is directly measured in the simulations. Note finally that in the strong confinement regime, that is, tubes with radii below 0.5 nm, one may not define a first layer anymore and the above picture cannot be applied. However due to the mainly 1D structure of water in this regime, a similar reasoning as above can be conducted, leading to a result similar to eq 3, but with the structure factor $S(\tilde{\mathbf{q}}_\pm)$ replaced by the 1D structure factor of water $S(q_{||,z})$ calculated at a wave vector $q_{||,z}$ along the longitudinal z direction, Figure 3b.

The relationship in eq 3 is checked in Figure 4b, showing a very good agreement between the numerical results for the friction coefficient and the predicted behavior: the variation of the friction coefficient is found to correlate directly with the previously defined structural parameters.

A key point is that the above relationship is able to reproduce the dependence of the friction coefficient versus the tube curvature, that is, a decrease of λ versus R for water inside, and an increase for water outside. For large radii (say $R > 2$ nm) the R dependence stems mainly from $S(\tilde{q}_{||})$; the change in structure factor $\Delta S = S(\tilde{q}_{||})(R) - S(\tilde{q}_{||})(R = \infty)$ is roughly proportional to the algebraic curvature R^{-1}, thus explaining the decreasing friction inside tubes and the increasing friction outside. However, inside CNTs, both roughness amplitude of the water−carbon potential $\tilde{f}_{q_{||}}$ and water contact density ρ_1 also contribute significantly, especially for smaller radii (see Supporting Information, Figure 7).

Physically the dependence on R originates from a curvature dependence of the energy landscape felt by water molecules, as sketched in Figure 5; while the structure of water is barely modified by curvature, the graphitic structure projected on the first water layer exhibits a curvature-induced shift. Depending on the CNT radius, the water feels a different graphitic potential map. For the smallest radii, the energy landscape of the carbon structure is furthermore smoothed out by curvature and the water molecules are transported within a flat, roughness-free, channel. This explains the extremely low friction undergone by water in this strong confinement regime where the water structure is close to single file.

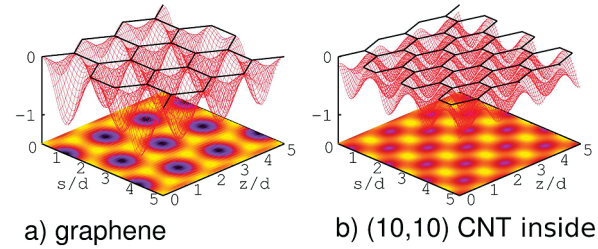

FIGURE 5. Curvature effects on the interaction energy landscape felt by a single water molecule in the first layer close to the carbon structure, computed from a direct summation of the water−carbon interaction at a distance σ from the carbon structure. The potential inside a curved CNT exhibits both a structural change and a smoothing of the potential wells.

Altogether, the effect of curvature can be illustrated by a naive analogy with an egg carton. When it is rolled on the inside, the structure is compressed in the orthoradial direction, and the wells of the landscape are smoothed. When it is rolled on the outside, the opposite effect happens.

The intimate connection of friction to water structure factor (computed at the CNT reciprocal wave vectors) suggests a potential dependence of friction on CNT chirality. We have checked this point by measuring the friction coefficient of water versus R inside a zigzag tube, instead of an armchair tube. The friction coefficient differs for the two chiralities for tubes with radius below 3 nm in a way that can be consistently explained with the above description (see Supporting Information Figure 9).

Conclusions. In this work, we have explored the friction of water in carbon nanotubes. Overall, our detailed study shows that the friction of water at graphitic surfaces exhibits a strong curvature dependency. By a careful analysis of the detailed physical mechanisms at the origin of liquid/solid friction, we have put forward a curvature-induced mismatch of the graphitic versus water structure, associated with an "incommensurability" of the water versus graphitic interface and leading to an extremely low liquid/solid friction for the smallest tubes. These theoretical findings supports the reported experimental results on fast transport of water in CNT with nanometric diameter.[4]

We quote that the friction coefficient is indeed the relevant physical parameter for transport in low friction channels. In a channel with a slip length much larger than the tube radius, associated with pluglike flow, the tube permeability, K, relating the flow rate $Q \simeq \pi R^2 V$ to the pressure gradient, $-\nabla P$, is found to reduce to

$$K = \frac{\pi R^3}{2\lambda} \qquad (4)$$

independently of the water viscosity. This relation can be obtained, without any assumption on hydrodynamic flow equations, by balancing the exact surface stress $\sigma_{wall} =$

DOI: 10.1021/nl1021046 | Nano Lett. 2010, 10, 4067–4073

$-R\nabla P/2$ to the solid/liquid friction force (per unit area) $F/\mathcal{A} = \lambda V$ (with $V \simeq V_{slip}$ for $b \gg R$). This surface-dominated regime of hydrodynamic permeability is to be compared with the "bulk" hydrodynamic behavior scaling as $K_{hydro} \sim R^4/\eta$.

Finally, our numerical results show that the friction coefficient of water inside armchair CNT vanishes, within numerical uncertainty, below a threshold diameter (Figure 2). We note that this specific behavior cannot be only ascribed to the incommensurability of the water−carbon structure; in contrast to the case of solid-on-solid friction,[27] the structure factor of the liquid computed at the roughness wave vector does not vanish. Therefore whether this vanishing friction arises from a true transition or a slow decrease beyond measurable values still remains uncertain within the present simulations and requires a dedicated study. It would be in any case important to understand the specific origin of this "transition" in order to, possibly, be able to tune the threshold radius to larger values.

Finally, the mechanisms highlighted in this paper are strongly linked with the structure of water. This suggests that molecules with different shapes may behave quite differently. In this context, the theoretical model reported in this paper should be able to tackle the question of flows of different liquids (alcohols, alkanes) in different types of nanotubes.

Altogether our results provide a firmly grounded fundamental understanding for the fast water transport in CNTs. This definitely confirms the power of nanofluidic devices as a key building block for future applications in ultrafiltration, desalination, energy conversion, and so forth.

Acknowledgment. L.B. acknowledges support from ANR under program P3N. RRN acknowledges financial support from the Elitenetzwerk Bayern (CompInt) and the Excellence Cluster Nano-Initiative Munich (NIM).

Supporting Information Available. Simulation details, weak confinement, strong confinement, and various tests. This material is available free of charge via the Internet at http://pubs.acs.org.

REFERENCES AND NOTES

(1) Sparreboom, W.; van den Berg, A.; Eijkel, J. C. T. *Nat. Nanotechnol.* **2009**, *4*, 713.
(2) Bocquet, L.; Charlaix, E. *Chem. Soc. Rev.* **2010**, *39*, 1073.
(3) Majumder, M.; Chopra, N.; Andrews, R.; Hinds, B. J. *Nature* **2005**, *438*, 44.
(4) Holt, J. K.; et al. *Science* **2006**, *312*, 1034.
(5) Whitby, M.; Cagnon, L.; Thanou, M.; Quirke, N. *Nano Lett.* **2008**, *8*, 2632.
(6) Kolesnikov, A. I.; et al. *Phys. Rev. Lett.* **2004**, *93*, No. 035503.
(7) Sui, H. X.; Han, B. G.; Lee, J. K.; Walian, P.; Jap, B. K. *Nature* **2001**, *414*, 872.
(8) Thomas, J. A.; McGaughey, A. J. H. *Nano Lett.* **2008**, *8*, 2788.
(9) Bocquet, L.; Barrat, J. L. *Soft Matter* **2007**, *3*, 685.
(10) Alexiadis, A.; Kassinos, S. *Chem. Rev.* **2008**, *108*, 5014.
(11) Hanasaki, I.; Nakatani, A. *J. Chem. Phys.* **2006**, *124*, 144708.
(12) Hummer, G.; Rasaiah, J. C.; Noworyta, J. P. *Nature* **2001**, *414*, 188.
(13) Sokhan, V. P.; Nicholson, D.; Quirke, N. *J. Chem. Phys.* **2002**, *117*, 8531.
(14) Gong, X.; Li, J.; Lu, H.; Zhang, H.; Fang, H. *Phys. Rev. Lett.* **2008**, *101*, 257801.
(15) Joseph, S.; Aluru, N. R. *Nano Lett.* **2008**, *8*, 452.
(16) Thomas, J. A.; McGaughey, A. J. H. *Phys. Rev. Lett.* **2009**, *102*, 184502.
(17) Berezhkovskii, A.; Hummer, G. *Phys. Rev. Lett.* **2002**, *89*, No. 064503.
(18) Cornell, W. D.; et al. *J. Am. Chem. Soc.* **1995**, *117*, 5179.
(19) Werder, T.; Walther, J. H.; Jaffe, R. L.; Halicioglu, T.; Koumoutsakos, P. *J. Phys. Chem. B* **2003**, *107*, 1345.
(20) Plimpton, S. *J. Comput. Phys.* **1995**, *117*, 1.
(21) van der Spoel, D.; Lindahl, E.; Hess, B.; Groenhof, G.; Mark, A. E.; Berendsen, H. J. C. *J. Comput. Chem.* **2005**, *26*, 1701.
(22) Español, P.; Zuniga, I. *J. Chem. Phys.* **1993**, *98*, 574.
(23) Bocquet, L.; Barrat, J. L. *Phys. Rev. E* **1994**, *49*, 3079.
(24) Huang, D. M.; Sendner, C.; Horinek, D.; Netz, R. R.; Bocquet, L. *Phys. Rev. Lett.* **2008**, *101*, 226101.
(25) Hansen, J. P.; Verlet, L. *Phys. Rev.* **1969**, *184*, 151.
(26) Barrat, J. L.; Bocquet, L. *Faraday Discuss.* **1999**, *112*, 119.
(27) Dienwiebel, M.; et al. *Phys. Rev. Lett.* **2004**, *92*, 126101.
(28) Simulations with flexible and fixed walls were shown to give similar results for the statics and friction of confined liquids;[10,16,19] flexibility increasing flow by a small (10−20%) and systematic amount.[13,15]
(29) Viscosity was measured independently in Couette flow simulations in the slab geometry. No significant change of viscosity has been measured for confinements larger than two water layers between the walls, confirming previous results.[2]

DOI: 10.1021/nl1021046 | *Nano Lett.* **2010,** *10,* 4067–4073